

Backstepping-based Robust Control for WMR with A Boundary in Prior for the Uncertain Rolling Resistance

M. Yue, S. Wang, X.L. Yang

Ming Yue*, Shuang Wang, Xiaoli Yang

School of Automotive Engineering

Dalian University of Technology, Dalian 116024, China

*Corresponding author: yueming@dlut.edu.cn

Abstract: In this study, we focus on the trajectory tracking control problem of a wheeled mobile robot (WMR) in an uncertain dynamic environment. Concerning the fact that the upper boundary may be usually achieved in prior according to the physical properties of the terrain, this crucial message is utilized to construct the controllers. Firstly, a dynamic model for WMR including the rolling resistance is presented, whose state variables are longitudinal and rotational velocities, as well as the rotational angle of the mobile platform. Secondly, with the aid of backstepping technique, the robust controllers based on the upper boundary are proposed and the globally asymptotic stability of the closed-loop system is proven by the Lyapunov theory in the following. Lastly, a saturation function is applied to replace the signum function, by which the inherent chattering can be suppressed greatly. Numerical simulation results demonstrate that the proposed controllers with upper bound in prior possess robustness characteristics which yields potentially valuable applications for the mobile robot, especially in the unstructured environment.

Keywords: Wheeled Mobile Robot (WMR), boundary estimation, uncertain rolling resistance.

1 Introduction

In practice, the physical properties of the wheeled mobile robot (WMR) within an unstructured environment are seldom considered in lots of trajectory tracking control issues. Among these physical properties, the rolling resistance acting on the robot wheels is such a crucial physical behavior that can effect the control performances greatly. Particular, in some rough terrain, such as loose soil and sand conditions, it is difficult to obtain high-performance of trajectory tracking without considering the influences of the rolling resistance. Therefore, when the WMR explores in an outdoor environment and even planetary surface, the rolling resistance may not be neglected for designing the system controllers [1].

Many efforts are devoted to the rolling resistance acting on the WMR's wheels recently. Most References (see [2,3]) had investigated the interactions of soil and wheels and then some new mechanical structures had also been reported to enhance the contact between the wheels and terrain. However, there are only a few investigations to deal with rolling resistance problem by control methods. After analysing of the terrain properties, we notice that the boundary (especially for the upper bound) of off-road rolling resistance can be calculated in advance according to the geologic parameters when the terrain of the exploration is determined. For practical implementation, the rolling resistance appears drastically changing, which is similar to the disturbances to the mobile benchmark, but with the aid of the boundary message in prior, the robust controller for WMR can be designed to make it possible to against the uncertain dynamics directly. It should be mentioned that, compared with modifying the system mechanical structure, the adopted control approach yields much more flexibility for the mobile robot. Certainly, we are also aware of adaptive scheme to update the upper bound, but the control algorithm with adaptive scheme

may make the regulation process more elastic and cause further time-delay usually [4, 5]. To overcome this drawback, a powerful robust control approach is determine to employ to deal with the uncertain problem of the unavoidable rolling resistance.

On another hand, if the rolling resistance is concerned, the dynamics of the WMR must be considered. For the past decades, most efforts have been done to the WMR with nonholonomic constraint on kinematic model, all of which the system velocities were assumed to be the control inputs [6, 7]. But unfortunately, there are only a few researches address the dynamic behaviors of nonholonomic system, where control inputs are transformed to be the system actuators, i.e., in most cases the driving torques of motors [8–10]. Since the rolling resistance is described in torque form when it takes place in practice, the dynamic properties must be considered when designing the system controllers to overcome this kind of uncertain dynamics.

With a widely survey of the current dynamic models for the WMR, we observe that a dynamic model proposed by Watanabe et.al [11] is so succinct and effective to describe the relationship between the rolling resistance and robot posture on the level of dynamics. Then, we utilize this dynamic model to establish the control system in this investigation. Particularly, it should be noted that the rolling resistance is somewhat difference from the external disturbances and unmodeled dynamics, because the rolling resistance lies in the movement process around a constant value; while the external disturbances and unmodeled dynamics possess white noise property which is around zero. The objective of this study is to address the rolling resistance behaviors of the WMR in detail, and derives the dynamic model to discuss the influence of rolling resistance. Based on addressed dynamic model, a simple and effective approach to stabilize the trajectory tracking system via backstepping techniques is developed. In order to illustrate the efficacy of the control approach, numerical simulations for a practical WMR have been performed.

2 WMR dynamics

The typical WMR can be described in Fig.1. It is assumed that the mobile robot is driven by two independent wheels as well as a passive auxiliary wheel is adopted to support the workbench. To begin with, some notations is introduced to help the controlling system design, as follows: l is the distance between the driving wheels and the symmetry axis; d is the distance between point $C(x, y)$ and the mass center of the robot $P(x_c, y_c)$, which is assumed to be on the symmetry axis; r is the radius of the driving wheels; m_p and m_w are the masses of vehicle body and wheel; I_c is the inertia moment of vehicle body w.r.t. vertical axis through C ; I_w and I_m are the inertia moments for the wheel w.r.t. wheel axis and diameter, respectively. According to the parallel axis theorem, the equivalent mass $m = m_p + 2m_w$ and rotation inertia $I = 2I_m + 2m_w l^2 + m_c d^2 + I_c$ can be introduced for simply.

The robot position can be described by the coordinates (x, y) , which is the midpoint C of the axis of two robot wheels, and the orientation angle ϕ , which is heading angle of body coordinate with respect to fixed frame (see Fig.1). With the hypothesis of *pure rolling and non slipping* condition, the nonholonomic constraint, i.e., $\dot{x} \sin \phi - \dot{y} \cos \phi = 0$, hold throughout the movements.

Let v and w be represent the linear and angular velocities of the mobile robot, and τ_r and τ_l express the driving torque of the right and left wheels, respectively. Through the analysis of the forces acting on the mobile robot, we can obtain that

$$I\ddot{\phi} = \frac{\tau_r}{r}l - \frac{\tau_l}{r}l \tag{1}$$

$$m\dot{v} = \frac{\tau_r}{r} + \frac{\tau_l}{r} \tag{2}$$

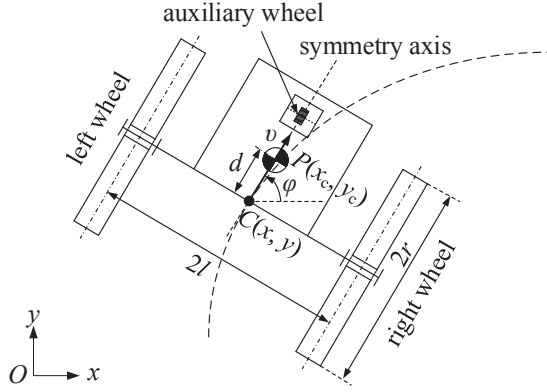


Figure 1: A wheeled mobile robot

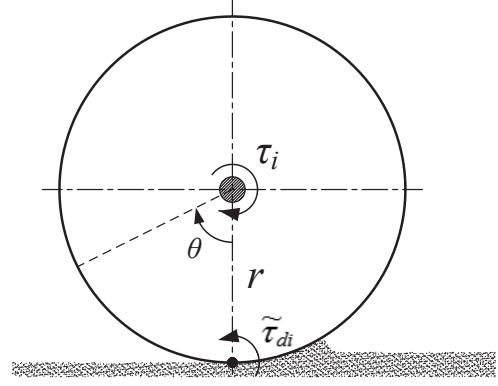


Figure 2: Rolling resistance generation

While rolling on the ground, especially operating on the soft soil or sandy terrain, the robot will suffer unavoidable rolling resistance, as shown in Fig.2. Let the notation $\tilde{\tau}_d$ represent this rolling resistance, and the dynamic behaviors of the wheel can be governed by

$$I_w \ddot{\theta}_i + c \dot{\theta}_i = k u_i - \tau_i - \tilde{\tau}_{di} \quad (3)$$

where τ_i is the driving input of the wheel (i expresses r or l for left or right wheels, the same hereinafter); c is the viscous friction coefficient and θ is the rolling angle of the wheel; k is driving gain between the motor's voltage and its output torque; u_i is the excited voltage signals for the motor installed in the relative wheel.

Let v_r, v_l denote the right and left linear velocity of the wheel center, and we can further have $v_r = r \dot{\theta}_r = v + l \dot{\phi}$ and $v_l = r \dot{\theta}_l = v - l \dot{\phi}$. Then, the relationship between linear velocity of the robot's platform and angular velocity of the robot wheels can be formulated by $r(\dot{\theta}_r + \dot{\theta}_l) = 2v$ and $r(\dot{\theta}_r - \dot{\theta}_l) = 2l \dot{\phi}$.

With the analysis, we can ultimately obtain the dynamics described by the linear velocity v and orientation angle ϕ as follows:

$$\dot{v} = -\frac{2cv}{mr^2 + 2I_w} + \frac{kr}{mr^2 + 2I_w}(u_r + u_l) - \frac{r}{mr^2 + 2I_w}(\tilde{\tau}_{dr} + \tilde{\tau}_{dl}) \quad (4)$$

$$\ddot{\phi} = -\frac{2cl^2}{Ir^2 + 2I_w l^2} \dot{\phi} + \frac{kr l}{Ir^2 + 2I_w l^2}(\tilde{\tau}_{dr} - \tilde{\tau}_{dl}) \quad (5)$$

If the system state variables are chosen as $x = [v \ \phi \ \dot{\phi}]^T$, the driving input is selected as $u = [u_r \ u_l]^T$, the disturbance vector is defined as $\tilde{\tau}_d = [\tilde{\tau}_{dr} \ \tilde{\tau}_{dl}]^T$, and the output variables are $y = [v \ \phi]^T$, a new dynamic model for control system design can be rewritten by:

$$\begin{cases} \dot{x} = Ax + Bu + D\tilde{\tau}_d \\ y = Cx \end{cases} \quad (6)$$

with

$$A = \begin{bmatrix} a_1 & 0 & 0 \\ 0 & 0 & 1 \\ 0 & 0 & a_2 \end{bmatrix}, \quad B = \begin{bmatrix} b_1 & b_1 \\ 0 & 0 \\ b_2 & -b_2 \end{bmatrix}, \quad D = \begin{bmatrix} d_1 & d_1 \\ 0 & 0 \\ d_2 & -d_2 \end{bmatrix}, \quad C = \begin{bmatrix} 1 & 0 & 0 \\ 0 & 1 & 0 \end{bmatrix},$$

where $a_1 = -\frac{2c}{mr^2 + 2I_w}$, $a_2 = -\frac{2cl^2}{Ir^2 + 2I_w l^2}$, $b_1 = \frac{kr}{mr^2 + 2I_w}$, $b_2 = \frac{kr l}{Ir^2 + 2I_w l^2}$, $d_1 = -\frac{r}{mr^2 + 2I_w}$, $d_2 = -\frac{r l}{Ir^2 + 2I_w l^2}$.

3 Control system design

3.1 System decoupling

Noticing that the system (6) is a coupled system, for the convenience of designing the system controller, the proposed dynamic model should be decoupled in the first place. To achieve this objective, a new control input vector should be introduced as follow:

$$\begin{bmatrix} u_r \\ u_l \end{bmatrix} = \begin{bmatrix} 1 & -1 \\ 0 & 1 \end{bmatrix} \begin{bmatrix} u_1 \\ u_2 \end{bmatrix} \quad (7)$$

With these modified inputs u_1 and u_2 , the system (6) is transformed into two independent subsystems:

$$\dot{v} = a_1 v + b_1 u_1 + \tilde{\tau}_{dv} \quad (8)$$

$$\dot{w} = a_2 w + b_2 u_1 - 2b_2 u_2 + \tilde{\tau}_{dw} \quad (9)$$

where $\tilde{\tau}_{dv} = d_1(\tilde{\tau}_{dr} + \tilde{\tau}_{dl})$ and $\tilde{\tau}_{dw} = d_2(\tilde{\tau}_{dr} + \tilde{\tau}_{dl})$, which represent disturbances for the two independent subsystems.

Supposing the robot moves on a special terrain ground, although the rolling resistance is in a changeable state, the maximum amplitude for $\tilde{\tau}_{dr}$ and $\tilde{\tau}_{dl}$ could be estimated in advance from the terrain property. Let the notation $\bar{\tau}_{dr}$ and $\bar{\tau}_{dl}$ represent the upper bound values of $\tilde{\tau}_{dr}$ and $\tilde{\tau}_{dl}$ respectively, and then it can be achieved that

$$\bar{\tau}_{dv} = \max |d_1(\tilde{\tau}_{dr} + \tilde{\tau}_{dl})| \quad (10)$$

$$\bar{\tau}_{dw} = \max |d_2(\tilde{\tau}_{dr} + \tilde{\tau}_{dl})| \quad (11)$$

3.2 Control scheme design

Considering the decoupled form of the system (8) and (9), a backstepping technique can be applied to derive the robot controller due to the high dimension feature of the system. The process of control design procedures may be divided into two steps which is given as bellows.

Step 1. Linear velocity control

After the trajectory tracking system has been decoupled, the control algorithms for linear and angular velocities can be derived stage by stage. Here, the control input u_1 is used to control the linear velocity, such that the robot can track an desired trajectory from an arbitrary original point with the required performances. Suppose that the desired linear velocity v_d , and the tracking error may be expressed by $v_e = v_d - v$. Then, a theorem can be given as follow:

Theorem 1. *For the linear velocity system (4) with the bounded linear velocity, the tracking error v_e will globally converge to zero, i.e., $\lim_{t \rightarrow \infty} v_e(t) = 0$, if the control law is given by*

$$u_1 = \frac{1}{b_1} [\dot{v}_d - a_1 v + c_1 v_e + \text{sgn}(v_e) \bar{\tau}_{dv}] \quad (12)$$

where c_1 is a positive constant and $\text{sgn}(\cdot)$ is a signum function.

Proof: Consider a candidate Lyapunov function as

$$V_1 = \frac{1}{2} v_e^2 \quad (13)$$

Differentiating V_1 with respect to time yields

$$\dot{V}_1 = v_e \dot{v}_e = v_e(\dot{v}_d - a_1 v - b_1 u_1 - \tilde{\tau}_{dv}) \quad (14)$$

Substituting (12) into (14), it can be ultimately obtained $\dot{V}_1 = -c_1 v_e^2 \leq 0$. Obviously, by Lyapunov stability theorem, the propose Theorem 1 is proved. \square

Step 2. Angular velocity control

Let ϕ_d represents the desired orientation angle of the robot to be tracked. Then, the tracking error of the orientation angle can be defined as $\phi_e = \phi_d - \phi$ and $\dot{\phi}_e = \dot{\phi}_d - \dot{\phi}$. In terms of angular velocity tracking control, it is to design the control input u_2 such that the ϕ_e and $\dot{\phi}_e$ converge to zero as $t \rightarrow \infty$. In order to realize this purpose, two virtual control inputs are introduced, which are defined as $z_1 = \phi_e$ and $z_2 = \dot{\phi}_e + c_2 \phi_e$ where c_2 is an arbitrary positive constant. Similar to the linear velocity control, based on the above definitions, a Theorem could be given as

Theorem 2. For the angular velocity system (5) with the bounded angular velocity, the tracking error ϕ_e and $\dot{\phi}_e$ will both globally converge to zero simultaneously, i.e., $\lim_{t \rightarrow \infty} \|\phi_e \ \dot{\phi}_e\| = 0$, if the control law is given by

$$u_2 = \frac{1}{2b_2} [a_2 w + b_2 u_1 - \ddot{\phi}_d - c_2 z_1 + c_3 z_2 + \text{sgn}(z_2) \bar{\tau}_{dw}] \quad (15)$$

where c_3 is a positive constant and $\text{sgn}(\cdot)$ is a signum function.

Proof: Consider a candidate Lyapunov function as

$$V_2 = \frac{1}{2} z_1^2 \quad (16)$$

Differentiating V_2 with respect to time achieves

$$\dot{V}_2 = z_1 \dot{z}_1 = z_1(\dot{\phi} - \dot{\phi}_d) = z_1 z_2 - c_2 z_1^2 \quad (17)$$

Notice that only Lyapunov function V_2 can not guarantee the global stability of the system. In order to stabilize the system, another virtual input z_2 is designed such that the entire tracking errors converge to zero. Hence, another candidate Lyapunov function constructed by z_2 is established for this purpose. The new candidate Lyapunov function is put forward as

$$V = \frac{1}{2} z_1^2 + \frac{1}{2} z_2^2 \quad (18)$$

Differentiating V with respect to time obtains

$$\dot{V} = \dot{V}_2 + z_2 \dot{z}_2 = z_1 z_2 - c_2 z_1^2 + z_2(a_2 w + b_2 u_1 - 2b_2 u_2 + c_2 \dot{z}_1 - \ddot{\phi}_d) \quad (19)$$

Substituting (12) and (15) into (19), one can obtain that $\dot{V} = -c_2 z_1^2 - c_3 z_2^2 \leq 0$. Obviously, according to Lyapunov stability theorem, the Theorem is proved. \square

Since the systems (8) and (9) are decoupled, the proposed controller (12) and (15) may guarantee the stabilization of the linear and angular velocity subsystems overall. To sum up, we can summarize the investigation results and ultimately give a theorem as follow:

Theorem 3. For the trajectory tracking system (4) and (5), the tracking errors v_e , ϕ_e and $\dot{\phi}_e$ will all globally converge to zero, i.e., $\lim_{t \rightarrow \infty} \|v_e \ \phi_e \ \dot{\phi}_e\| = 0$, with the controller (12) and (15).

The proof can be easily achieved according to the above analysis.

From the controller designing process, it can be observed that the candidate Lyapunov functions are established step by step, which make the control design process be simple and convenience. This is a backstepping approach which is usually applied for controller design of a sophisticated nonlinear systems. Meanwhile, it should be emphasized that there are inherent chattering caused by signum function $\text{sgn}(\cdot)$ in the proposed controllers. To overcome this drawback, one can replace signum function $\text{sgn}(\cdot)$ by saturation functions $\text{sat}(\cdot)$ to suppress this behaviors, one of which can be given by:

$$\text{sat}(\chi) = \frac{\chi}{|\chi| + \epsilon} \tag{20}$$

where ϵ is a positive constant and χ represents arbitrary variable.

4 Simulation results

In this section we perform numerical simulations to verify the effectiveness of the proposed controllers. The simulated parameters of the mechanical structure of the WMR are supposed to be $m_c = 14\text{kg}$, $m_w = 3\text{kg}$, $I_c = 0.9\text{kgm}^2$, $I_m = 0.05\text{kgm}^2$, $I_w = 0.015\text{kgm}^2$, $l = 0.3\text{m}$, $d = 0.05\text{m}$, $r = 0.1\text{m}$, $k = 0.95$, and $c = 0.01$. From the required performance of the trajectory tracking, the control parameters as selected as follows: $c_1 = c_2 = c_3 = 10$ and $\epsilon = 0.002$. Suppose the mobile robot starts from initial point $[x \ y \ \phi]^T = [0 \ 0 \ 0]^T$; meanwhile, the desired trajectory of linear and angular velocity are hypothesized to be $v_d = 1\text{m/s}$, $w_d = \sin t$ with the initial state vector $x_0 = [v_0 \ \phi_0 \ w_0]^T = [0.5 \ 0.2 \ 0]^T$. Moreover, the rolling resistance acting on the left and right wheels are supposed to be a worse situation in simulation than that in practice to verify the effectiveness of the control algorithms. So a synthesis signal consisted of two sinusoid signals with different frequency is introduced to imitate the rolling resistance. Here, assume that the rolling resistances are same on the left and right wheels, i.e., $\tilde{\tau}_{dr} = \tilde{\tau}_{dl} = \sin w_d t + \sin 2w_d t$ where w_d denotes the resistance frequency. According to practical experiment, the $\tilde{\tau}_{dr}$ and $\tilde{\tau}_{dl}$ can be set as the value of 0.75Nm and 3Nm respectively in this simulation circumstance. In addition, the saturation should be considered for actual driving motor, so a maximum value 10Nm is introduced to restrict the control outputs, i.e., $|\tau_r| \leq 10\text{Nm}$ and $|\tau_l| \leq 10\text{Nm}$.

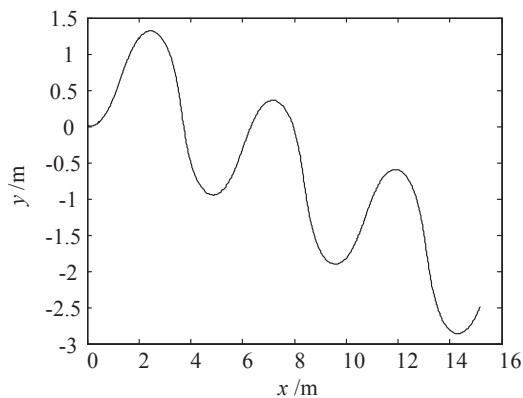


Figure 3: Actual trajectory on the plane

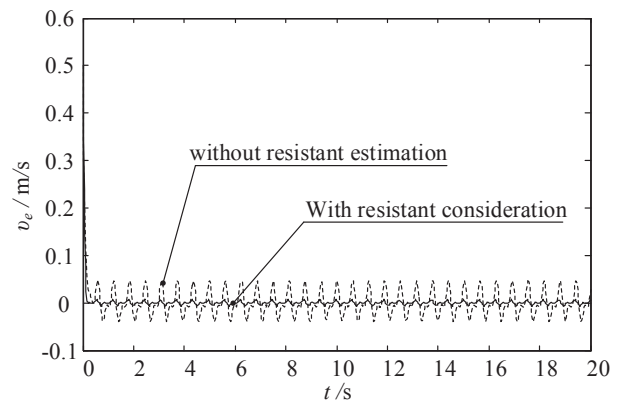


Figure 4: Tracking error for v_e

Under the proposed simulation circumstance, the actual tracking process for the desired trajectory is plotted in Fig.3. It indicates the proposed control method can make the mobile robot to track the desired trajectory with satisfactory tracking performances. Besides, we simulate two cases, that is, with and without estimation, to illustrate the signification of control with and

without upper bound information. As shown in Fig.4, the tracking error relative to the linear velocity without boundary is described as the dashed line, as well as the case with boundary is plotted by the dashed line. The results state the tracking errors become much smaller (reduced to 20% of the amplitude) when $\bar{\tau}_{dv}$ and $\bar{\tau}_{dw}$ are adopted. Particularly, owing to the $\text{sat}(\cdot)$, the inherent chattering is also suppressed. Lower chattering may be achieved with smaller ϵ , but it will cause more violent changes for the control inputs.

Furthermore, to exhibit the better tracking performance with the upper bound, the tracking errors of $\dot{\phi}_e$ and ϕ_e are also addressed in Fig.5 and Fig.6, respectively. It is observed that the amplitudes of ϕ_e and w_e are reduced to 21% and 18% nearly compared with the case without upper bound estimation, which yields that the derived controller can provide better performances for tracking system and the robustness is enhanced in the following.

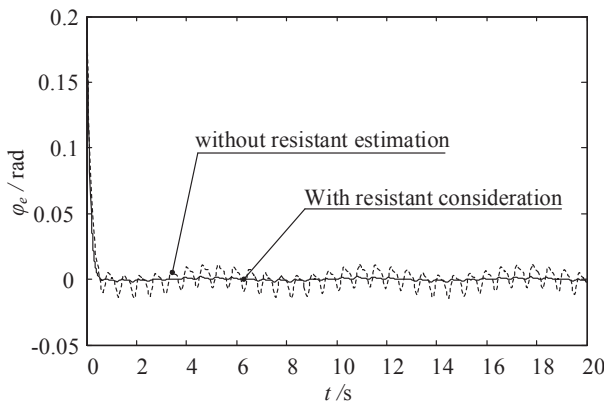


Figure 5: Tracking errors for ϕ_e

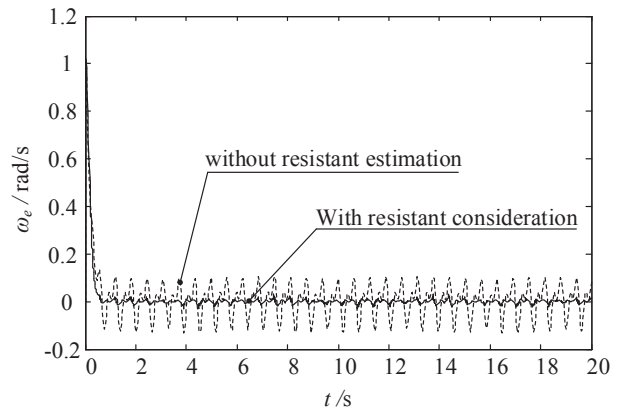


Figure 6: Tracking errors for ω_e

5 Conclusions

The trajectory tracking issues were discussed in this study, and the main contribution can be summarized as follows: 1) a decoupled dynamic model was used to describe the complicated nonlinear behaviors of WMR where the rolling resistances are concerned. The decoupled model consisted of two parts: a first-order model for linear velocity and a second-order model for orientation angle of the robot, which not only kinematic postures but also dynamics behaviors were all included; 2) based on the fact that the upper bound of rolling resistance which can be achieved in prior, a robust controller was developed to obtain the better tracking performances. The backstepping methodology was employed to derive the system controller considering the higher dimensional property of the tracking system; and 3) a saturation function was introduced to alleviate the inherent chattering caused by signum function. Such treatment was simply but effective for a practical WMR system.

Acknowledgement

This research was supported by grants from the National Natural Science Foundation of China (No. 61175101), and the Fundamental Research Funds for the Central Universities (No. DUT12LK45).

Bibliography

- [1] L. Ding, H. B. Gao, Z. Q. Deng, K. Nagatani, and K. Yoshida, Experimental study and analysis on driving wheels performance for planetary exploration rovers moving in deformable soil, *Journal of Terramechanics*, 48(1): 27-45, 2011.
- [2] C. C. Ward and K. Iagnemma, A dynamic-model-based wheel slip detector for mobile robots on outdoor terrain, *IEEE Transactions on Robotics*, 24(4): 821-831, 2008.
- [3] P Lamon and R. Siegwart, Wheel torque control in rough terrain-modeling and simulation, *IEEE Int. Conf. on Robotics and Automation*, Barcelona, Spain, 867-872, 2005.
- [4] X. M. Sun, G. P. Liu, W. Wang and D. Rees, L_2 -gain of systems with input delays and controller temporary failure: Zero-order hold model, *IEEE Transactions on Control Systems Technology*, 19(3): 699-706, 2011.
- [5] R. Wang, G. P. Liu, W. Wang, D. Rees and Y. B. Zhao, H_∞ control for networked predictive control systems based on the switched Lyapunov function method, *IEEE Transactions on Industrial Electronics*, 57(10): 3565-3571, 2010.
- [6] A. Chatterjee, O. Ray, A. Chatterjee and A. Rakshit, Development of a real-life EKF based SLAM system for mobile robots employing vision sensing, *Expert Systems with Applications*, 38(7): 8266-8274, 2011.
- [7] D. Bucciari, D. Perritaz, P. Mullhaupt, Z. P. Jiang and D. Bonvin, Velocity-scheduling control for a unicycle mobile robot: Theory and experiments, *IEEE Transactions on Robotics*, 25(2): 451-458, 2009.
- [8] Z. J. Li and S. Z. S. Ge and A. G. Ming, Adaptive robust motion/force control of holonomic-constrained nonholonomic mobile manipulators, *IEEE Transactions on Systems, Man, and Cybernetics, Part B: Cybernetics*, 37(3): 607-616, 2007.
- [9] M. Yue, P. Hu and W. Sun, Path following of a class of non-holonomic mobile robot with underactuated vehicle body, *IET Control Theory and Applications*, 4(10): 1898-1904, 2009.
- [10] M. Yue, W. Sun and P. Hu, Sliding mode robust control for two-wheeled mobile robot with lower center of gravity, *International Journal of Innovative Computing Information and Control*, 7(2): 637-646, 2011.
- [11] K. Watanabe, J. Tang, M. Nakamura, S. Koga and T. Fukuda, Fuzzy-Gaussian neural network and its application to mobile robot control, *IEEE Transactions on Control Systems Technology*, 4(2): 193-199, 1996.